

The fundamental thumb-tip force vectors produced by the muscles of the thumb

Jonathan L. Pearlman^a, Stephanie S. Roach^a, Francisco J. Valero-Cuevas^{a,b,*}

^a *Neuromuscular Biomechanics Laboratory, Sibley School of Mechanical and Aerospace Engineering, Cornell University, 222 Upson Hall, Ithaca, NY 14853-7501, USA*

^b *Laboratory for Biomedical Mechanics and Materials, Hospital for Special Surgery, New York, NY, USA*

Received 8 January 2003

Abstract

A rigorous description of the magnitude and direction of the 3D force vector each thumb muscle produces at the thumb-tip is necessary to understand the biomechanical consequences to pinch of a variety of paralyses and surgical procedures (such as tendon transfers). In this study, we characterized the 3D force vector each muscle produces at the thumb-tip, and investigated if these thumb-tip force vectors scaled linearly with tendon tension. In 13 cadaver specimens, we measured the output 3D thumb-tip force vector produced by each tendon acting on the thumb, plus two common tendon transfers, as a function of input tendon tension. After fixing the hand to a rigid frame, we mounted the thumb by configuring it in standardized key or opposition pinch posture and coupling the thumb-tip to a rigidly held 6 degree-of-freedom force/torque sensor. Linear actuators applied tension to the distal tendons of the four extrinsic thumb muscles, and to six Nylon cords reproducing the lines of action of (i) the four intrinsic thumb muscles and (ii) two alternative tendon transfers commonly used to restore thumb opposition following low median nerve palsy. Each computer-controlled linear actuator ramped tendon tension from zero to 1/3 of predicted maximal muscle force expected at each tendon, and back to zero, while we measured the 3D force vector at the thumb-tip. In test/re-test trials, we saw thumb-tip force vectors were quite sensitive to mounting procedure, but also sensitive to variations in the seating of joint surfaces. We found that: (i) some thumb-tip force vectors act in unexpected directions (e.g., the *opponens* force vector is parallel to the distal phalanx), (ii) the two tendon transfers produced patently different force vectors, and (iii) for most muscles, thumb-tip force vectors do not scale linearly with tendon tension—likely due to load-dependent viscoelastic tendon paths, joint seating and/or bone motion. Our 3D force vector data provide the first quantitative reference descriptions of the thumb-tip force vectors produced by all thumb muscles and two tendon transfers. We conclude that it may not be realistic to assume in biomechanical models that thumb-tip force vectors scale linearly with tendon tensions, and that our data suggest the thumb may act as a “floating digit” affected by load-dependent trapezium motion.

© 2003 Orthopaedic Research Society. Published by Elsevier Ltd. All rights reserved.

Keywords: Hand; Finger; Thumb; Cadaveric; Surgical planning; Muscle coordination

Introduction

The force vectors produced at the thumb-tip by individual thumb muscles have not been previously quantified, even though these data would be instrumental in describing how muscle forces manifest themselves as thumb-tip force vectors in the healthy, paralyzed, and

post-operative thumb. Available descriptions of the biomechanical function of thumb muscles and their tendons include quantitative measures of muscle parameters including moment arms (i.e., the perpendicular distance between the force line of action and the joint center) and muscle architecture (e.g., fiber length, physiological cross-sectional area (PCSA)) [3,5,14]. Unfortunately, muscle parameters do not translate directly or unequivocally into descriptions of the 3D force vector each muscle produces at the thumb-tip—where pinch forces occur and where force vectors need to be restored after low median nerve palsy, for example. Similarly, the graphical description of the lines of action of intact and transferred tendons at each joint has been of limited use

* Corresponding author. Address: Neuromuscular Biomechanics Laboratory, Sibley School of Mechanical and Aerospace Engineering, Cornell University, 222 Upson Hall, Ithaca, NY 14853-7501, USA. Tel.: +1-607-255-3575; fax: +1-607-255-1222.

E-mail address: fv24@cornell.edu (F.J. Valero-Cuevas).

URL: <http://www.mae.cornell.edu/valero>

to represent the biomechanical function of muscles at the thumb-tip, to predict deficit after paralysis, and to compare alternative tendon transfers. These Cartesian plots of the moment generating capacity of a muscle about each joint it crosses [3,14] are created by combining the lines of action of tendons with respect to the anatomical structures (e.g., joint axes, other tendons, etc.) with PCSA and moment arm data. These plots distill the complex anatomical lines of actions muscles into manageable diagrams describing the torque a muscle or tendon transfers could produce about specific joint axes. However, these plots cannot be unequivocally extrapolated to find the force vector a tendon transfer produces at the thumb-tip.

Importantly, the above descriptions of the biomechanical function of thumb muscles rely on accurate and realistic estimates of moment arms [2]—but the validity of moment arm measurements depends on technical skill and realistic assumptions about the number, location and orientation of the joint axes of the thumb, which remains debatable (cf. [9] vs. [5]). In addition, there may be inter-subject variability and load-dependent deformation of tendon paths or motion of the carpal bones, especially the trapezium [3], which are not accounted for in any kinematic model of the thumb or measurements of moment arms. Note that moment arms have been measured by applying tendon tension of at most 10% of the strength of thumb muscles (i.e., 2 N [14]), even though some thumb muscles can produce forces up to 100 N [5]. It is also important to note that the transformation from muscle forces to thumb-tip force vectors is assumed to be linear in biomechanical models [1,8,16], in spite of the deformation ligaments and tendons can undergo under physiologic loads [3,17] due to their viscoelastic properties.

In this study, we expand on a previously described system identification approach [15,18] to address two questions: (i) What is the 3D magnitude and direction of the force vector each muscle produces at the thumb-tip? (ii) Do thumb-tip force vectors scale linearly with tendon tension for realistic tension magnitudes? Unlike the available descriptions of the biomechanical function of thumb muscles, this approach does not make any assumptions about the kinematic structure of the thumb because it directly measures the thumb-tip force vectors that arise when known tensions are applied along the lines of action of the muscles of cadaveric thumbs. We also provide an example of a clinical application of this approach by measuring the thumb-tip force vectors produced by two tendon transfers.

Methods

As in previous studies of the index finger [15,18] and thumb [13], we began by dissecting the intrinsic and extrinsic muscles acting in the

thumb of 13 fresh-frozen forearm specimens (7 males, 6 females, Age = 76 ± 9 years). Specimens were pre-screened for blood-borne pathogens and kept moist with a mixture of bovine serum (10%, product #C6278, Sigma Chemical Company, St. Louis, MO) and water during the entire dissection and experiment. We isolated and removed from their origins the extrinsic muscle bellies: (flexor pollicis longus (FPL), extensor pollicis longus (EPL), extensor pollicis brevis (EPB), and abductor pollicis longus (AbPL)). After excising the muscles bellies, we tied and glued (Vetbond Tissue Adhesive, 3M Inc., St. Paul, MN) 1-mm Nylon cords to the each tendon. Next, we isolated and removed from their origin the intrinsic muscles of the thenar eminence: abductor pollicis brevis (AbPB), flexor pollicis brevis (FPB), and opponens pollicis (OPP). We tied and glued Nylon cords to the AbPB and FPB at their insertions (Fig. 1h and j, respectively). The muscle belly of the OPP was completely excised, and an eyehook (3-mm ID) was screwed flush to the surface of the first metacarpal at the OPP insertion (Fig. 1f). Other eyehooks were screwed flush into the trapezium and trapezoid at the origins of the AbPB and OPP, respectively, and were used to route the Nylon cords (Fig. 1i and g, respectively). A floating 3-mm ring tied around the proximal end of the third metacarpal was used to represent the origin of the FPB (in the palmar fascia (Fig. 1k). After dissection of the thenar muscles, we excised the belly of the adductor pollicis (ADD). We screwed an eyehook into the proximal-ulnar aspect of the proximal phalanx at the ADD origin (Fig. 1a). Because of the fan-shape of the ADD, we represented the muscle with two Nylon cords. The ADD oblique (ADD_o) cord was routed through an eyehook placed in the capitate (Fig. 1c), and the ADD transverse (ADD_t) was routed through an eyehook placed in the distal end of the palmar aspect of the third metacarpal (Fig. 1b); these eyehooks were placed at the extreme proximal and distal locations of the ADD origin to represent all of the possible actions (by vector addition) of the fan-shaped ADD. The first dorsal interosseous (DIO) was isolated and excised and eyehooks were placed in the ulnar aspect of the first metacarpal (at mid-shaft) and in the radial aspect of the head of the second metacarpal at the origin and insertion of the DIO, respectively (Fig. 1d and e). We also routed two tendon transfers commonly used for low median nerve palsy [7]:

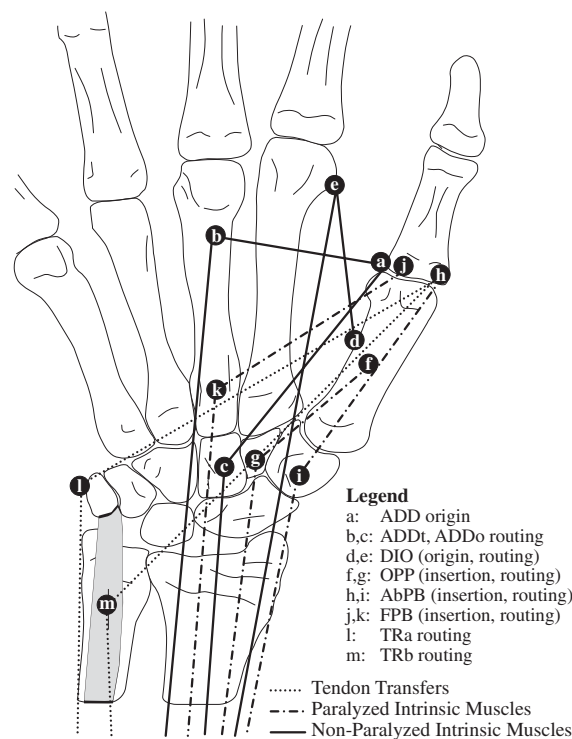


Fig. 1. Representative schematic dissection diagram showing the approximate eyehook location and lines of action of the intrinsic muscle and tendon transfer cords.

transfer A (TRa), attributed to Burkhalter et al., is performed by transferring the *extensor indicis proprius* muscle to the insertion of the failed AbPB via the pisiform bone, and transfer B (TRb), attributed to Riordan, is performed by transferring the flexor digitorum superficialis (FDS) of the ring finger to the insertion of the failed AbPB via a slip in the flexor carpi ulnaris (FCU) (Fig. 1l and m, respectively). In the cases where we used eyehooks to represent the origin of the muscles (ADD, OPP and DIO) we tied the Nylon cord to the base of the eyehook (rather than the eye itself) to ensure that the cord was in contact with the bone, mimicking the tendinous origin coming out of the bone. Tendon paths were left covered by skin to avoid drying out of the tendon sheaths.

After the dissection, we used an external fixation device (Agee-WristJack, Hand Biomechanics Lab, Inc., Sacramento, CA) to fix the second and third metacarpals to the radius and ulna in neutral wrist flexion/extension and radial/ulnar deviation [15,18]. We then configured the thumb in two functional postures using a manual goniometer: key pinch (10° interphalangeal (IP) flexion, 45° metacarpophalangeal (MP) flexion, and 0° carpometacarpal (CMC) abduction and flexion) and opposition pinch (45° IP flexion, 10° MP flexion, 45° CMC abduction, and 0° CMC flexion). We formed thermoplastic molds (Omega Max, North Coast Medical Inc., Morgan Hill, CA) for each of these postures to hold the thumb in position while it was mounted to a custom table-top load frame. The aluminum load frame housed ten linear actuators, each consisting of a stepper motor (model 801B-AM, American Scientific Instrument Corp., Palos Hills, IL) mounted in-line with a uniaxial load cell (SML series ± 107.5 N or ± 215 N, depending on the strength of the muscle simulated, InterfaceForce, Scottsdale, AZ) and an extension spring (to increase the resolution of force control). We mounted the specimen on the load frame by configuring it in standardized key or opposition pinch posture. As in our *in vivo* studies [10,16,19], the thumb interfaced with a rigidly held 6 degree-of-freedom force/torque sensor (F/T nano17, ATI/Industrial Automation, Garner, NC) via a thermoplastic thimble formed around the distal phalanx. The thimble was rigidly connected to the sensor and glued to the thumb pulp to keep the thumb-tip in the thimble (Fig. 2, inset). The mixed boundary conditions of the thimble-thumb interface (soft-tissue interface for palmar, radial, ulnar, and distal force production, and a rigid interface of the thumbnail and thimble during dorsal force production) are our well established method of noninvasively measuring 3D digit-tip force production *in vivo* [10,16,19] that allow for the natural compliance of soft-tissue.

A personal computer (Celeron, Dell Computer Corporation, Round Rock, Texas) with a data acquisition card (DAQ PCI 6021E, National Instruments Corporation, Austin, TX) running custom pro-

grams in LabVIEW (National Instruments Corporation, Austin, TX) controlled the linear actuators attached to each tendon's Nylon cord.

After mounting the specimen, we measured the output force vector at the thumb-tip when tension was applied to each tendon. We commanded each linear actuator to incrementally ramp tension up from zero to a desired value and back down to zero from that value in ten ramp-and-hold steps in each direction under force control (precision: ± 0.05 N). We recorded thumb-tip output force vector during hold periods to exclude actuator vibrations. We did not analyze the torque vector produced at the thumb-tip because it is beyond the scope of this work. The maximum force for each muscle was based on the mass fraction reported in the literature [3] and was scaled so that each muscle reached approximately 1/3 of its maximal predicted force based on PCSA (Table 1, FMAX column; note, FMAX was assumed to be identical for both postures). Prior work showed that tendon tensions greater than 40 N would risk rupture of the attachment of the tendon to the Nylon cord [15,18].

We calculated two measures of *intra*-specimen reproducibility by calculating the percent magnitude difference and included angle between thumb-tip output force vectors for each muscle across two test/re-test trials. For the 1st reproducibility measure, we repeated ramp-up and down trials for all muscles after decoupling the thumb-tip from the dynamometer, moving the thumb randomly through its range of motion and re-coupling the thumb-tip *without moving the dynamometer*. This quantified the sensitivity of thumb-tip force vectors to any joint seating variations that may occur after articulating the thumb and reattaching the thimble in the *identical* position and orientation as the first trial. For the 2nd reproducibility measure, we repeated trials after re-doing the entire mounting procedure: we placed the posture mold on the thumb (holding it in the approximate desired key or opposition pinch posture), decoupled the dynamometer, and moved the dynamometer to a random location and back, intending to re-attach the thimble to the dynamometer at the same thumb posture and thimble position and orientation as the first trial. This quantified the sensitivity of thumb-tip force vectors to the mounting procedure, excluding the creation of the thermoplastic posture molds, but *including* joint seating variations that may have occurred due to changes in the spatial relationships between bones after reconnecting the thumb-tip to the re-positioned dynamometer.

We used three measures to quantify the relationship between input tendon tensions and output thumb-tip force vectors. (i) We found the fundamental action of each muscle at the thumb-tip by calculating an average 3D thumb-tip force vector in both magnitude and direction across tension levels for each tendon for each specimen and averaged across specimens. (ii) We characterized the degree of association

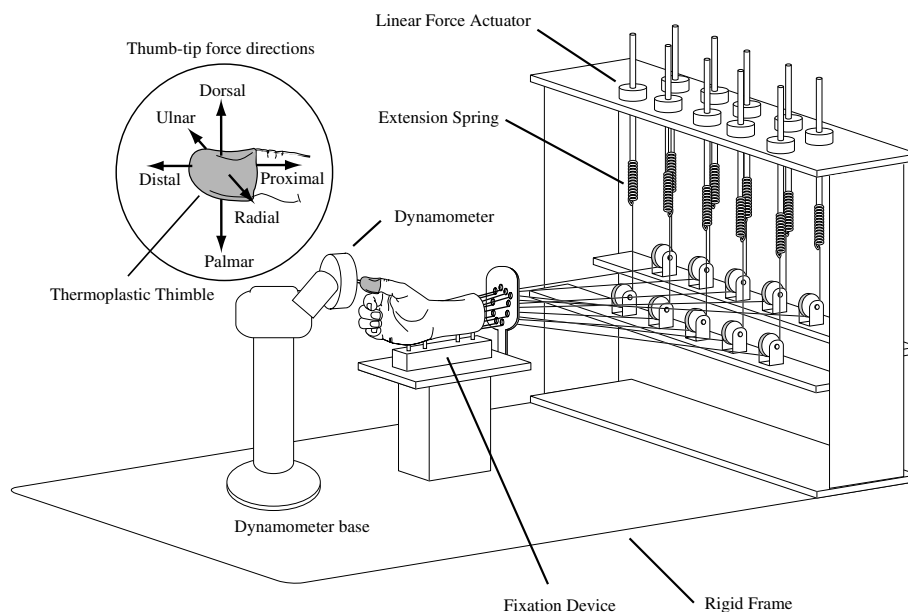


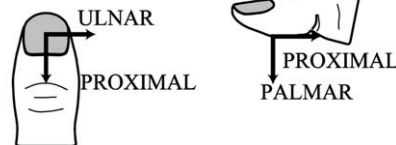
Fig. 2. Computer-controlled loading apparatus.

Table 1
Nonlinearity and average thumb-tip force vector results

| Muscle | FMAX | Key pinch | | | | | Opposition pinch | | | | | | | | |
|------------------|------|-----------|------|------|------|-----------|------------------|---------|-----|------|------|------|-----------|---------|---------|
| | | %NL | PLM | ULN | PRX | $\ F\ $ | DSL PRJ | RAD PRJ | %NL | PLM | ULN | PRX | $\ F\ $ | DSL PRJ | RAD PRJ |
| AbPB | 10.5 | 85 | 0.5 | -1.5 | 0.5 | 1.7 (0.6) | 44 | 30 | 85 | 0.4 | -1.4 | 0.3 | 1.5 (0.9) | 46 | 33 |
| AbPL | 30 | 91 | 0.1 | -2.0 | 5.0 | 5.3 (1.5) | 56 | 56 | 90 | 0.1 | -0.8 | 3.1 | 3.2 (0.8) | 56 | 57 |
| ADD _o | 14.4 | 100 | 2.1 | 0.6 | -1.9 | 2.9 (1.0) | 55 | 50 | 100 | 2.5 | 0.4 | -1.6 | 3.0 (0.9) | 33 | 45 |
| ADD _t | 14.4 | 100 | 1.3 | 1.3 | -4.1 | 4.5 (1.8) | 56 | 54 | 100 | 1.3 | 1.4 | -3.3 | 3.9 (1.4) | 55 | 55 |
| DIO | 12.6 | 100 | -0.1 | 0.2 | -1.4 | 1.4 (0.9) | 56 | 53 | 100 | 0.0 | 0.5 | -1.1 | 1.2 (0.7) | 48 | 50 |
| EPB | 7.8 | 92 | -0.9 | -0.3 | 0.7 | 1.2 (0.3) | 33 | 43 | 92 | -1.0 | -0.1 | 0.7 | 1.2 (0.4) | 34 | 42 |
| EPL | 12.6 | 92 | -0.9 | 1.6 | 0.2 | 1.9 (0.5) | 50 | 35 | 75 | -1.1 | 1.3 | 0.1 | 1.7 (0.5) | 48 | 43 |
| FPB | 12.6 | 92 | 1.1 | 0.0 | -1.3 | 1.7 (0.8) | 27 | 43 | 100 | 0.7 | -0.1 | -1.4 | 1.6 (0.7) | 38 | 44 |
| FPL | 26.1 | 50 | 5.6 | -0.5 | 4.5 | 7.2 (0.9) | 53 | 57 | 44 | 5.8 | -0.9 | 3.9 | 7.0 (1.5) | 55 | 57 |
| OPP | 18.3 | 92 | -0.2 | -0.3 | -2.4 | 2.4 (1.2) | 53 | 52 | 100 | -0.1 | -0.2 | -2.3 | 2.3 (1.3) | 51 | 50 |
| TR _a | 9.6 | 100 | 0.1 | -0.6 | -3.2 | 3.3 (2.2) | 56 | 54 | 100 | -0.1 | -0.7 | -2.8 | 2.9 (2.1) | 56 | 54 |
| TR _b | 19.4 | 90 | 0.7 | -2.0 | -2.2 | 3.1 (1.7) | 49 | 42 | 92 | 0.2 | -2.1 | -1.8 | 2.8 (1.7) | 49 | 38 |

DORSAL VIEW

RADIAL VIEW



In all specimens, the tension in each tendon was ramped up from zero to its FMAX (N) level in ten equal steps, and then ramped down to zero in ten steps. The FMAX applied to each tendon was based on published PCSA values [3,4] and maximal muscle stress of 35.4 N/cm² [4,6,12,20]. %NL is the percentage of regression cases of tendon tensions against each of the three thumb-tip force components that were nonlinear. These thumb-tip force vector components (averaged across tension levels and specimens, and scaled to $\|F\|$) in the palmar (PAM), ulnar (ULN), and proximal (PRX) orthogonal directions (*N*) are reported as if all hands were right hands. $\|F\|$ is the magnitude (*N*) (mean(SD)) of the force vectors at their maximal force values (FMAX). PRJ columns indicate the orientation variability (SD in degrees) from the mean direction of the thumb-tip force vectors in the dorsal (DSL) and radial (RAD) views (see inset).

between input tendon tension and the Euclidean magnitude of the output thumb-tip force vector by calculating the square of their Pearson product-moment correlation coefficient (r^2). And (iii) we tested the linearity of the transformation from tendon tension to thumb-tip force magnitude by regressing the tendon tensions (*X*) against each of the three force components (in the palmar-ulnar-proximal reference frame; Fig. 2, inset) of the thumb-tip output vector (*Y*) using a quadratic model ($Y = a_0 + a_1 * X + a_2 * X^2$). An *F*-test ($\alpha = 0.05$) determined if the quadratic term (a_2) was significantly different from zero. Only if the null hypothesis ($H_0 : a_2 = 0$) could not be rejected in all three force directions would we conclude that the thumb-tip output force vector scaled linearly with tendon tension. Otherwise, we concluded that the response was significantly different from linear.

Results

The average 3D thumb-tip force vectors produced by all thumb muscles are shown in Fig. 3 and Table 1. See www.mae.cornell.edu/nmb1/thumb/avgvec.html for an interactive three-dimensional exploration of results for opposition posture.

The high degree of association between tendon tension and magnitude of the thumb-tip output force vector is shown by the box plots showing all r^2 values across postures and specimens across muscles (Fig. 3, box plots).

The output thumb-tip force vector was nonlinearly related to input tendon tension in most cases (Table 1,

%NL column), suggesting that a quadratic or higher-order relationship is needed to describe how thumb-tip force vectors scale with tendon tension.

Regarding reproducibility of the experiment when we articulated the thumb (without moving the dynamometer), the thumb-tip output force changed in magnitude by $4 \pm 18\%$ and direction by $9 \pm 10^\circ$ compared to the initial trial. This suggests the experiment was sensitive to the seating of the joints. When remounting the thumb and re-positioning the dynamometer, the thumb-tip output force magnitude changed an average of 35% with respect to the first test (standard deviation (SD) = 77%), and vector direction changed by an average of 34° (SD = 34°). This suggests the experiment was highly sensitive to the combined effects of joint seating and mounting procedure.

Discussion

In multi-joint musculoskeletal systems such as the thumb, a muscle generates torque at each joint it crosses that is proportional to the muscle’s force and moment arm. The force and torque output at a finger-tip in static pinch depends on the net torque at each joint produced

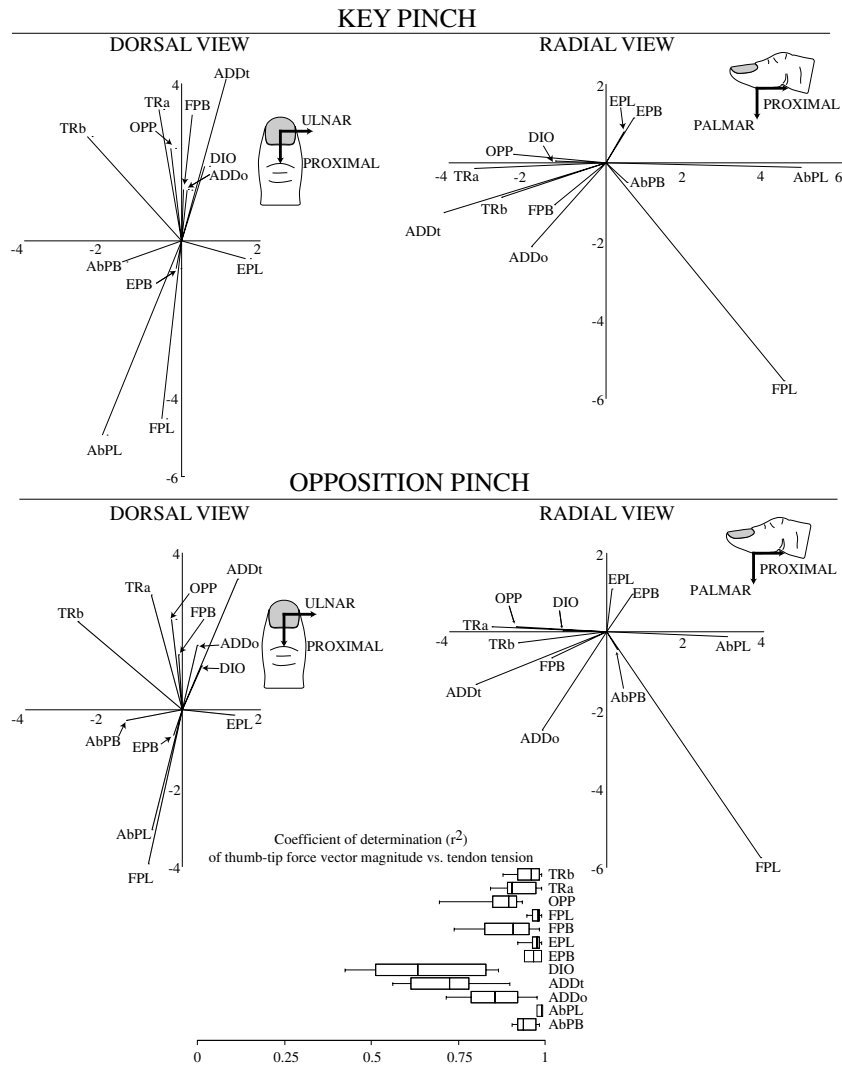


Fig. 3. Average thumb-tip output vectors (N) for each functional posture in anatomical projections. All data were rotated to a right hand. For an interactive three-dimensional exploration of results for opposition posture see www.mae.cornell.edu/nmb1/thumb/avgvec.html. We also show the r^2 values of thumb-tip force vector Euclidean magnitude vs. tendon tension for each muscle across postures and specimens.

by the combined action of all active muscles, and the geometry and configuration of the skeletal structure of the finger [16,19]. Because of the thumb’s complex anatomy, it is difficult to predict with certainty the thumb-tip output each thumb muscle produces [16]. In this study, we characterized the thumb-tip force vectors produced by each muscle of the thumb and two tendon transfers by directly applying known tensions to the tendons of cadaver thumbs and measuring the resulting force output at the thumb-tip.

The average 3D thumb-tip force vectors describe how the actions of tendon tensions span the possible 3D force-producing directions at the thumb-tip without having made assumptions about the underlying biomechanical system (e.g. kinematic structure [15,18]); Fig. 3, Table 1, and www.mae.cornell.edu/nmb1/thumb/avgvec.html. These graphs, tables, and interactive web-

site will complement the available descriptions of the actions of thumb muscles [3,11,14] by presenting the 3D description of the vector force produced by individual muscles at the thumb-tip. Additionally, we reported the actions of two common tendon transfers for low median palsy, allowing for easy comparison of their thumb-tip force vectors with respect to the available and paralyzed musculature.

Because we found that thumb-tip vectors are non-linearly related to tendon tension, our study is limited in that these average force vectors are valid up to the 1/3 of maximum muscle force regime and extrapolating to higher tendon tensions may not be valid. Given that most functional manipulation occurs at sub-maximal force levels, our results are, nevertheless, representative of realistic requirements of thumb function. In addition, the routing of the Nylon cords, including the

visual placement of eyehook screws, may not have accurately reproduced the paths of some muscles. Additionally, activity in one muscle may affect the line of action of another muscle, such as when the activity in the OPP may cause the AbPB to separate from the thumb CMC joint (increasing its moment arm [3]). Applying tension to multiple muscles simultaneously may result in increased nonlinearity. We are currently exploring the nonlinearity of thumb-tip force vectors when several tendons are loaded simultaneously. Lastly, our two measurements of *intra*-specimen reproducibility suggest thumb-tip output force vectors are sensitive to both joint seating and mounting procedure. The small changes in the force vectors ($4 \pm 18\%$ and $9 \pm 10^\circ$ in magnitude and direction, respectively) when the thumb-tip was returned to the same position and orientation after moving the thumb (1st reproducibility measure) can be reasonably attributed to differences in the seating of thumb joints because the skeletal column of the thumb may have more than 6 degree-of-freedom due to the soft-tissue at the thumb pad, and the kinematic complexity and inherent laxity of the joints of the thumb. That is, fixing the position and orientation of the thimble and hand did not guarantee that all joints would be seated in the same way before and after moving the thumb. The much larger changes in the force vectors ($35 \pm 77\%$ and $34 \pm 34^\circ$ in magnitude and direction, respectively) when re-positioned the thumb and dynamometer (2nd reproducibility measure) show the results to be highly sensitive to the compounded effects of joint seating and mounting procedure. In future, we will use robotic manipulators (as in [15,18]) and 3D motion analysis to improve thumb posture and mounting accuracy, but need to retain the use of the thimble to allow compatibility with *in vivo* studies.

Our results do demonstrate that the thumb-tip force vector magnitudes are strongly associated with tendon tension ($r^2 > 0.8$), with DIO and ADDt having lower r^2 values, but >0.5 (Fig. 3, box plots). Moreover, the correlation between the thumb-tip force vector direction and tendon tension is best modeled by a nonlinear function (Table 1, %NL column). The nonlinear behavior of the system, assuming negligible deformation of the bone, is likely due to load-dependent viscoelastic tendon paths, joint seating and/or bone motion. We were careful to use stiff 200 N test Nylon cord and rigid frames to eliminate the likelihood that our loading apparatus could introduce nonlinear deflection artifacts. The nonlinear relationships we found between input tendon tension and output thumb-tip force vectors challenges the common assumption used for biomechanical models of the thumb that this relationship is linear [1,8,16]. We are currently exploring the extent to which these nonlinearities affect the motor control of the thumb.

Load-dependent proximal motion of the trapezium is a likely contributor to the nonlinearity of thumb-tip force vector production. In our preliminary experiments, where we pinned the distal phalanx of the thumb to the dynamometer (as in [15,18]), we noticed thumb-tip force vectors progressively swung proximally and rapidly increased in magnitude as tendon tension increased. Careful examination showed that the trapezium migrated proximally when tendon tensions were applied, therefore causing the thumb-tip to “hang” from the dynamometer. We, thus, used a thimble to allow physiologic compliance at the thumb-tip-dynamometer coupling, as in our *in vivo* studies [10,16,19], to allow the joints to remain seated. While this may have added variability, thereafter the output force vectors no longer swung proximally.

Load-dependent motion has been reported elsewhere for the trapezium [3] and carpus in general [17], but no quantitative measures of this motion have been reported. Even though this study was not designed or equipped to reliably measure trapezium motion, we confirmed trapezium motion in two specimens (with a rigidly coupled thumb-tip) by measuring the displacement of a pin inserted in the trapezium (using digital video close-ups) as a function of FPL tension. We found this motion to be ~ 2.0 mm in the proximal direction at maximal FPL tension, which likely underestimates the trapezium motion compared to when more muscles are active. To exclude the possibility that our dissection of the intrinsic musculature led to trapezium laxity, we performed one additional experiment where we loaded FPL prior to the dissection of the intrinsic muscles, and noted a similar motion of a pin inserted in the trapezium. Thus we propose the thumb does not have a rigid base at the trapezium, but in reality acts as a “floating digit” affected by motion of the carpal bones when its tendons are loaded. This load-dependent displacement of the trapezium likely contributes to the nonlinear transmission of tendon tension by, at a minimum, affecting joint seating and configuration, which in turn affect the transformation of individual tendon tensions into thumb-tip force vectors. We are conducting additional *in vivo* Computed Tomography studies during static pinch to characterize the load-dependence of thumb kinematics, and quantify changes in joint kinematics, tendon paths and moment arms, if any.

Our work has several clinical implications. The nonlinearity of fingertip force production we found is clinically important because it calls into question the conventional method of quantifying the mechanical function of musculotendons. To describe the actions of muscles, researchers report tables of moment potentials [3,14], which reflect the mechanical advantage of the muscles about each joint they cross, and the maximum tendon tension predicted by PCSA. The nonlinearities in thumb-tip force production that we identified suggests

that the moment potentials may be related to force level in the muscle, and that the moment potentials reported in the literature represent only an instance of a continuous response to force. Researchers have only recorded the mechanical advantage of a muscle under only nominal tendon tensions (e.g., 2 N in [14]), thus moment arm data may not be representative of physiologically loaded tendons.

In addition, our work underscores how standard anatomical nomenclature can be of little value in describing fingertip force production for clinical restoration of function. Conventional anatomical nomenclature describes finger muscle actions from the perspective of individual joint movements: abductors abduct a given joint, while flexors flex a given joint. These names simply specify the dominant motion of the digit with tendon excursion, often while other joints are held fixed, and have little value in describing thumb-tip force production even in the isometric case (e.g., pinch). Our work complements anatomical nomenclature by providing functional descriptions of 3D force vectors at the thumb-tip—where pinch forces occur and where force vectors need to be restored clinically. Using a reference frame fixed on the thumb tip (Fig. 2, inset) we note, for example, that the thumb-tip action of ADDo and ADDt is greater in the distal and palmar directions than in the ulnar (“adduction”) direction, and that OPP acts almost purely in the distal direction (Fig. 3).

Lastly, our results demonstrate how alternative, but presumably equivalent, tendon transfers to restore thumb opposition can be compared and contrasted by analyzing the 3D thumb-tip output force they produce. When exploring the data interactively (see www.mae.cornell.edu/nmb/thumb/avgvec.html), and in the Dorsal Views of Fig. 3, it is clear that transfer B (TRb: transferring the ring finger FDS via a slip in the FCU) better reproduces the radial component of force lost after low median nerve palsy (i.e., previously provided by AbPB). This is but one example of how tendon transfers can be compared. In the future, other surgical procedures could be rigorously evaluated in this way.

Acknowledgements

This study was supported by a Whitaker Foundation Biomedical Research Grant (to FVC). This material is based upon work supported under a National Science Foundation Graduate Research Fellowship (to JLP). The Authors gratefully acknowledge that Michal Weisman built portions of the experimental apparatus; Drs. John Hermanson and Elizabeth Fisher provided help and laboratory space; and Madhusudhan Venkadesan, Veronica Santos, and Laurel Kuxhaus helped with the cadaver experiments.

References

- [1] An KN, Chao EY, Cooney WP, Linscheid RL. Forces in the normal and abnormal hand. *J Orthop Res* 1985;3:202–11.
- [2] An KN, Takahashi K, Harrigan TP, Chao EY. Determination of muscle orientations and moment arms. *J Biomech Eng* 1984; 106:280–2.
- [3] Brand P, Hollister A. *Clinical mechanics of the hand*. St. Louis, MO: Mosby-Year Book, Inc.; 1999. 369 pp.
- [4] Brand PW, Beach RB, Thompson DE. Relative tension and potential excursion of muscles in the forearm and hand. *J Hand Surg [Am]* 1981;6:209–19.
- [5] Chao EY. *Biomechanics of the hand a basic research study*. Singapore; Teaneck, NJ: World Scientific; 1989. 191 pp.
- [6] Close RI. The relations between sarcomere length and characteristics of isometric twitch contractions of frog sartorius muscle. *J Physiol* 1972;220:745–62.
- [7] Crenshaw AH, Daugherty K, Campbell WC. *Campbell’s operative orthopaedics*. 9th ed. St. Louis: Mosby Year Book; 1998. 4076 pp.
- [8] Giurintano DJ, Hollister AM, Buford WL, Thompson DE, Myers LM. A virtual five-link model of the thumb. *Med Eng Phys* 1995;17:297–303.
- [9] Hollister A, Giurintano DJ, Buford WL, Myers LM, Novick A. The axes of rotation of the thumb interphalangeal and metacarpophalangeal joints. *Clin Orthop* 1995:188–93.
- [10] Kuxhaus LC. Changes in thumb 3D force production with selective paralysis. MS Thesis. Sibley School of Mechanical and Aerospace Engineering, Cornell University, Ithaca, NY, 2003. 225 pp.
- [11] Lieber RL, Jacobson MD, Fazeli BM, Abrams RA, Botte MJ. Architecture of selected muscles of the arm and forearm: anatomy and implications for tendon transfer. *J Hand Surg [Am]* 1992; 17:787–98.
- [12] Powell PL, Roy RR, Kanim P, Bello MA, Edgerton VR. Predictability of skeletal muscle tension from architectural determinations in guinea pig hindlimbs. *J Appl Physiol* 1984;57:1715–21.
- [13] Roach SS, Short WH, Werner FW, Fortino MD. Biomechanical evaluation of thumb opposition transfer insertion sites. *J Hand Surg [Am]* 2001;26:354–61.
- [14] Smutz WP, Kongsayreepong A, Hughes RE, Niebur G, Cooney WP, An KN. Mechanical advantage of the thumb muscles. *J Biomech* 1998;31:565–70.
- [15] Valero-Cuevas FJ, Hentz VR. Releasing the A3 pulley and leaving flexor superficialis intact increase palmar force following the Zancolli lasso procedures to prevent claw deformity in the intrinsic minus hand. *J Orthop Res* 2002.
- [16] Valero-Cuevas FJ, Johanson ME, Towles JD. Towards a realistic biomechanical model of the thumb: the choice of kinematic description is more critical than the solution method or the variability/uncertainty of musculoskeletal parameters. *J Biomech* 2003;36:1019–30.
- [17] Valero-Cuevas FJ, Small CF. Load dependence in carpal kinematics during wrist flexion in vivo. *Clin Biomech* 1997;12:154–9.
- [18] Valero-Cuevas FJ, Towles JD, Hentz VR. Quantification of fingertip force reduction in the forefinger following simulated paralysis of extensor and intrinsic muscles. *J Biomech* 2000; 33:1601–9.
- [19] Valero-Cuevas FJ, Zajac FE, Burgar CG. Large index-fingertip forces are produced by subject-independent patterns of muscle excitation. *J Biomech* 1998;31:693–703.
- [20] Zajac FE. Muscle and tendon: properties, models, scaling, and application to biomechanics and motor control. *Crit Rev Biomed Eng* 1989;17:359–411.